

Pair Production and Correlated Decay of Heavy Majorana Neutrinos in e^+e^- Collisions

Axel Hofer* and L. M. Sehgal†

Institut für Theoretische Physik (E), RWTH Aachen

D-52074 Aachen, Germany

Abstract

We consider the process $e^+e^- \rightarrow N_1N_2$, where N_1 and N_2 are heavy Majorana particles, with relative CP given by $\eta_{CP} = +1$ or -1 , decaying subsequently via $N_1, N_2 \rightarrow W^\pm e^\mp$. We derive the energy and angle correlation of the dilepton final state, both for like-sign ($e^\mp e^\mp$) and unlike-sign ($e^- e^+$) configurations. Interesting differences are found between the cases $\eta_{CP} = +1$ and -1 . The characteristics of unlike-sign e^+e^- dileptons originating from a Majorana pair N_1N_2 are contrasted with those arising from the reaction $e^+e^- \rightarrow N\bar{N} \rightarrow W^+e^-W^-e^+$, where $N\bar{N}$ is a Dirac particle-antiparticle pair.

*email: hofer@physik.rwth-aachen.de

†email: sehgal@physik.rwth-aachen.de

I. INTRODUCTION

In an interesting paper [1], Kogo and Tsai have analysed the reaction $e^+e^- \rightarrow N_1N_2$, where $N_{1,2}$ are heavy Majorana neutrinos, and compared the cases where the relative CP of N_1 and N_2 is $\eta_{CP} = +1$ and -1 . It was found that the two cases differ in threshold behaviour, in angular distribution, and in the dependence on the spin-directions of N_1 and N_2 . A comparison was also made between the Majorana process and the Dirac process $e^+e^- \rightarrow N\bar{N}$, where $N\bar{N}$ is a Dirac particle-antiparticle pair. A related analysis was carried out in Ref. [2]. (The contrast between Majorana neutrinos and Dirac neutrinos has been the subject of several other papers (e.g. [3–6]) and monographs ([7,8]))

In the present paper, we examine how the differences between the cases $\eta_{CP} = +1$ and -1 propagate to the decay products of N_1 and N_2 , assuming the decays to take place via $N_{1,2} \rightarrow W^\pm e^\mp$. We focus on the like-sign lepton pair created in the reaction chain $e^+e^- \rightarrow N_1N_2 \rightarrow W^+e^-W^+e^-$, which is a characteristic signature of Majorana pair production. We derive, in particular, the correlation in the energies of the e^-e^- pair, and in their angles relative to the e^+e^- axis. Interesting differences are found between the cases $\eta_{CP} = +1$ and -1 . We also examine the behaviour of the unlike-sign dileptons e^+e^- , comparing the Majorana cases with dileptons created in the production and decay of a Dirac $N\bar{N}$ pair, i.e. $e^+e^- \rightarrow N\bar{N} \rightarrow W^+e^-W^-e^+$.

II. CHARACTERISTICS OF THE REACTION $e^+e^- \rightarrow N_1N_2$

The analysis of Ref. [1] was carried out in the context of the simple production mechanism for $e^+e^- \rightarrow N_1N_2$ shown in Fig. 1, and we begin by recapitulating the essential results. The interaction Lagrangian is taken to be

$$\begin{aligned} \mathcal{L}_1(x) = & -\frac{g}{2 \cos \theta_W} \left[\bar{e}(x) \gamma_\mu (c_V - c_A \gamma_5) e(x) \right. \\ & + \alpha_N \bar{N}_1(x) \gamma_\mu \frac{1}{2}(1 - \gamma_5) N_2(x) \\ & \left. + \alpha_N \bar{N}_2(x) \gamma_\mu \frac{1}{2}(1 - \gamma_5) N_1(x) \right] Z^\mu(x) \quad , \end{aligned} \quad (2.1)$$

where c_V , c_A and α_N may be regarded as real phenomenological parameters. (For the standard Z-boson, $c_V = -1/2 + 2 \sin^2 \theta_W$, $c_A = -1/2$). The matrix element for Majorana neutrinos (with momenta and spins as indicated in Fig. 1) is

$$\mathcal{M}_m = -i\alpha_N \left(\frac{g}{2 \cos \theta_W}\right)^2 j_\mu^e \Delta_Z^{\mu\nu} \left[\bar{u}_{t_1}(q_1) \gamma_\nu \frac{1}{2}(1 - \gamma_5) v_{t_2}(q_2) \lambda_2 - \bar{u}_{t_2}(q_2) \gamma_\nu \frac{1}{2}(1 - \gamma_5) v_{t_1}(q_1) \lambda_1 \right], \quad (2.2)$$

where

$$j_\mu^e = \bar{v}_{s_2}(p_2) \gamma_\mu (c_V - c_A \gamma_5) u_{s_1}(p_1) \quad (2.3)$$

and

$$\Delta_Z^{\mu\nu} = \frac{g^{\mu\nu} - q^\mu q^\nu / m_Z^2}{q^2 - m_Z^2 + i m_Z \Gamma_Z}. \quad (2.4)$$

Assuming CP -invariance the factors λ_1 , λ_2 in Eq. (2.2) are such that $\lambda_1 \lambda_2^* = +1(-1)$ when N_1 and N_2 have the same (opposite) CP -parity [9]. Rewriting the second term in Eq. (2.2) as

$$\bar{u}_{t_2}(q_2) \gamma_\nu \frac{1}{2}(1 - \gamma_5) v_{t_1}(q_1) = \bar{u}_{t_1}(q_1) \gamma_\nu \frac{1}{2}(1 + \gamma_5) v_{t_2}(q_2), \quad (2.5)$$

we observe that the current of the Majorana neutrinos is pure axial vector when N_1 and N_2 have the same CP -parity ($\eta_{CP} = \lambda_1 \lambda_2^* = +1$), and pure vector when they have opposite CP ($\eta_{CP} = \lambda_1 \lambda_2^* = -1$). In comparison, the matrix element for the Dirac process $e^+ e^- \rightarrow N \bar{N}$ is

$$\mathcal{M}_d = -i\alpha_N \left(\frac{g}{2 \cos \theta_W}\right)^2 j_\mu^e \Delta_Z^{\mu\nu} \bar{u}_{t_1}(q_1) \gamma_\nu \frac{1}{2}(1 - \gamma_5) v_{t_2}(q_2). \quad (2.6)$$

The differential cross section for $e^+ e^- \rightarrow N_1 N_2$, for general masses m_1 and m_2 , and for arbitrary polarizations \vec{n} and \vec{n}' of the two neutrinos is given in the Appendix. In Sec. 5 we compare our formulas with those of Ref. [1], and with special cases treated in other papers. Here we specialise to the case $m_1 = m_2 = m_N$, for which the cross-section ($d\sigma/d\Omega$) in the cases $\eta_{CP} = +1$ and -1 is

$$\left(\frac{d\sigma}{d\Omega}\right)_+ = \frac{1}{2}\sigma_0 \beta^3 \left\{ f_1 [(n_y n'_y - n_x n'_x)S^2 + (1 + n_z n'_z)(1 + C^2)] - f_2 2(n_z + n'_z)C \right\} , \quad (2.7)$$

$$\left(\frac{d\sigma}{d\Omega}\right)_- = \sigma_0 \beta \left\{ f_1 [2 - \beta^2 + C^2\beta^2 + n_z n'_z(\beta^2 + C^2(1/\gamma^2 + 1)) + n_x n'_x S^2(1/\gamma^2 + 1) - n_y n'_y S^2\beta^2 + (n_x n'_z + n'_x n_z)2SC/\gamma^2] - f_2 [2(n_x + n'_x)S/\gamma^2 + 2(n_z + n'_z)C] \right\} . \quad (2.8)$$

For comparison, the differential cross section of the Dirac process $e^+e^- \rightarrow N\bar{N}$ is

$$\begin{aligned} \left(\frac{d\sigma}{d\Omega}\right)_d = \frac{1}{2}\sigma_0 \beta \left\{ f_1 [(1 + C^2\beta^2) - (n_z + n'_z)\beta(1 + C^2) \right. \\ \left. - (n_x + n'_x)SC\beta/\gamma + n_z n'_z(C^2 + \beta^2) + (n_x n'_z + n_z n'_x)SC/\gamma + n_x n'_x S^2/\gamma^2] + \right. \\ \left. f_2 [2C\beta - (n_z + n'_z)C(1 + \beta^2) - (n_x + n'_x)S/\gamma + 2n_z n'_z C\beta + (n_x n'_z + n'_x n_z)S\beta/\gamma] \right\} . \end{aligned} \quad (2.9)$$

The symbols in Eqs. (2.7)–(2.9) are defined as follows:

$$\sigma_0 = \frac{G_F^2 \alpha_N^2}{512\pi^2} \left| \frac{m_Z^2}{s - m_Z^2 + im_Z \Gamma_Z} \right|^2 s \quad , \quad \beta = (1 - 4m_N^2/s)^{1/2} \quad , \quad \gamma = (1 - \beta^2)^{-1/2} \quad (2.10)$$

$$C = \cos \theta \quad , \quad S = \sin \theta \quad , \quad f_1 = 2(c_V^2 + c_A^2) \quad , \quad f_2 = 4c_V c_A \quad ,$$

θ being the scattering angle of N_1 (or N) with respect to the initial e^- direction. The co-ordinate axes are defined so that the momentum- and spin-vectors of N_1 and N_2 in the e^+e^- c.m. frame have the components

$$\begin{aligned} q_1^\mu = (\gamma m, 0, 0, \gamma \beta m) \quad , \quad t_1^\mu = (\gamma \beta n_z, n_x, n_y, \gamma n_z) \quad , \\ q_2^\mu = (\gamma m, 0, 0, -\gamma \beta m) \quad , \quad t_2^\mu = (-\gamma \beta n'_z, n'_x, n'_y, \gamma n'_z) \quad . \end{aligned} \quad (2.11)$$

Inspection of Eqs. (2.7)–(2.9) reveals several interesting features:

- (a) The Majorana cases '+' and '-' have different dependence on the spin-vectors \vec{n} and \vec{n}' , and different angular distributions, even after the spins \vec{n} and \vec{n}' are summed over. These differences stem from the fact that the matrix element \mathcal{M}_m in Eq. (2.2) effectively involves an axial vector current $\bar{N}_1 \gamma_\mu \gamma_5 N_2$ when $\lambda_1 \lambda_2^* = +1$ and a vector current $\bar{N}_1 \gamma_\mu N_2$ when $\lambda_1 \lambda_2^* = -1$.

- (b) The Majorana cases '+' and '-' differ from the Dirac case 'd', in which the current of the $N\bar{N}$ -pair has a V-A structure $\bar{N}\gamma_\mu\frac{1}{2}(1-\gamma_5)N$. This difference persists even if the spins of the heavy neutrinos are summed over, in which case

$$\begin{aligned}\sum_{\vec{n},\vec{n}'}\left(\frac{d\sigma}{d\Omega}\right)_+ &= 2\sigma_0\beta^3\left[f_1(1+C^2)\right], \\ \sum_{\vec{n},\vec{n}'}\left(\frac{d\sigma}{d\Omega}\right)_- &= 4\sigma_0\beta\left[f_1(2-\beta^2+C^2\beta^2)\right], \\ \sum_{\vec{n},\vec{n}'}\left(\frac{d\sigma}{d\Omega}\right)_d &= 2\sigma_0\beta\left[f_1(1+C^2\beta^2)+f_2(2C\beta)\right].\end{aligned}\tag{2.12}$$

Whereas the spin-averaged Majorana cross sections are forward-backward symmetric, the Dirac process has a term linear in $\cos\theta$, with a coefficient proportional to $f_2 = 4c_Vc_A$. Eq. (2.12) also shows that the threshold behaviour is β^3 , β and β for the cases '+', '-' and 'd' respectively. In the asymptotic limit $\beta \rightarrow 1$ the Majorana cases '+' and '-' have the same angular distribution $(1+C^2)$, distinct from that of the Dirac process.

- (c) In the high energy limit $\beta \rightarrow 1$, the Dirac process $e^+e^- \rightarrow N\bar{N}$ has a spin-dependence given by

$$\left(\frac{d\sigma}{d\Omega}\right)_d = \frac{1}{2}\sigma_0\beta\left[1-(n_z+n'_z)+n_zn'_z\right]\left[f_1(1+C^2)+2f_2C\right].\tag{2.13}$$

The fact that only the longitudinal components (n_z and n'_z) of the N, \bar{N} spins appear in this expression is consistent with the expectation that relativistic Dirac neutrinos are eigenstates of helicity. The fact that the cross section (2.13) vanishes when $n_z = -1$, $n'_z = +1$ confirms the expectation that for a V-A current the N and \bar{N} are produced in left-handed and right-handed states, respectively. By comparison, the Majorana processes $e^+e^- \rightarrow N_1N_2$, for $\eta_{CP} = +1$ and -1 , have the high energy behaviour ($\beta \rightarrow 1$)

$$\left(\frac{d\sigma}{d\Omega}\right)_+ = \frac{1}{2}\sigma_0\left\{f_1\left[(1+C^2)(1+n_zn'_z)+S^2(n_yn'_y-n_xn'_x)\right]-2f_2C(n_z+n'_z)\right\},\tag{2.14}$$

$$\left(\frac{d\sigma}{d\Omega}\right)_- = \frac{1}{2}\sigma_0 \left\{ f_1 [(1 + C^2)(1 + n_z n'_z) + S^2(n_x n'_x - n_y n'_y)] - 2f_2 C (n_z + n'_z) \right\}. \quad (2.15)$$

Contrary to the Dirac case, the Majorana reactions have an explicit dependence on n_x , n_y and n'_x , n'_y , reflecting the fact that a relativistic Majorana particle with $m_N \neq 0$ is not necessarily an eigenstate of helicity, and can have a spin pointing in an arbitrary direction. The Majorana cases '+-' and '-+' differ in the sign of the term proportional to S^2 , which contains the transverse (x- and y-) components of the neutrino spins. It is with the purpose of exposing the subtle differences in the spin state of the $N_1 N_2$ and $N \bar{N}$ systems that we investigate in the following sections the dilepton final state created by the decays of the heavy neutrinos via $N_{1,2} \rightarrow W^\pm e^\mp$ and $N(\bar{N}) \rightarrow W^+ e^- (W^- e^+)$.

III. LIKE-SIGN DILEPTONS: THE REACTION $e^+ e^- \rightarrow N_1 N_2 \rightarrow W^+ W^+ e^- e^-$

As seen in the preceding, the spin state and the angular distribution of the Majorana pair produced in $e^+ e^- \rightarrow N_1 N_2$ depends on the relative CP -parity η_{CP} of the two particles. We wish to see how these differences manifest themselves in the decay products of N_1 and N_2 . To this end, we assume that $m_N > m_W$, and that the simplest decay mechanism is $N_{1,2} \rightarrow W^\mp e^\pm$. In particular, the reaction sequence $e^+ e^- \rightarrow N_1 N_2 \rightarrow W^+ W^+ e^- e^-$ leads to the appearance of two like-sign leptons in the final state, an unmistakable signature of Majorana pair production. (For the purpose of this paper we assume that the W -bosons decay into quark jets, thus avoiding the complications of final states with 3 or 4 charged leptons.)

We have calculated the amplitude of the process $e^+ e^- \rightarrow N_1 N_2 \rightarrow W^+ W^+ e^- e^-$, depicted in Fig. 2, assuming a decay interaction (α'_N and α''_N being real parameters)

$$\begin{aligned} \mathcal{L}_2(x) = & -\frac{g}{\sqrt{2}} \left[\alpha'_N \bar{e}(x) \gamma_\mu \frac{1}{2}(1 - \gamma_5) N_1(x) W^{\mu-}(x) \right. \\ & + \alpha'_N \bar{N}_1(x) \gamma_\mu \frac{1}{2}(1 - \gamma_5) e(x) W^{\mu+}(x) \\ & \left. + \alpha''_N \bar{e}(x) \gamma_\mu \frac{1}{2}(1 - \gamma_5) N_2(x) W^{\mu-}(x) \right] \end{aligned}$$

$$+ \alpha''_N \bar{N}_2(x) \gamma_\mu \frac{1}{2}(1 - \gamma_5) e(x) W^{\mu+}(x) \quad \Big] . \quad (3.1)$$

This amplitude has the form (see Appendix for details)

$$\begin{aligned} \mathcal{M} = & iA \ j_\mu^e \ \Delta_Z^{\mu\nu} \frac{1}{q_1^2 - m_1^2 + im_1\Gamma_1} \cdot \frac{1}{q_2^2 - m_2^2 + im_2\Gamma_2} \cdot \\ & \left[m_2 \lambda_2 \bar{u}_{t_1}(k_1) \gamma_\rho \not{q}_1 \gamma_\nu \gamma_\sigma \frac{1}{2}(1 + \gamma_5) v_{t_2}(k_2) \right. \\ & \left. - m_1 \lambda_1 \bar{u}_{t_2}(k_2) \gamma_\sigma \not{q}_2 \gamma_\nu \gamma_\rho \frac{1}{2}(1 + \gamma_5) v_{t_1}(k_1) \right] \epsilon_{\lambda_3}^{*\rho}(k_3) \epsilon_{\lambda_4}^{*\sigma}(k_4) , \end{aligned} \quad (3.2)$$

where

$$A = \alpha_N \alpha'_N \alpha''_N \cdot \frac{g^4}{8 \cos^2 \theta_W} . \quad (3.3)$$

Using the narrow-width approximation for the N_1 , N_2 propagators, and specializing to the case $m_1 = m_2 = m_N$, we obtain the following expression for the squared matrix element (summed over final and averaged over initial spins), the subscript in \mathcal{M}_\pm denoting $\eta_{CP} = \pm 1$ ($q = p_1 + p_2$, $l = p_1 - p_2$):

$$\begin{aligned} |\overline{\mathcal{M}_\pm}|^2 = & \frac{|A|^2}{2} \frac{1}{(s - m_Z^2)^2} \frac{\pi}{m_N \Gamma_n} \delta(q_1^2 - m_N^2) \frac{\pi}{m_N \Gamma_n} \delta(q_2^2 - m_N^2) \frac{m_N^2}{m_W^4} \cdot \\ & \left\{ f_1 \cdot \left(\mp (m_N^2 - m_W^2)^2 (m_N^2 + 2m_W^2)^2 \cdot s \mp 4(m_N^2 - 2m_W^2)^2 \cdot \right. \right. \\ & \left[s (k_1 k_2)(q_1 q_2) - s (k_1 q_2)(k_2 q_1) - (k_1 k_2)(q_1 q)(q_2 q) + (k_1 k_2)(q_1 l)(q_2 l) \right. \\ & + (k_1 q_2)(k_2 q)(q_1 q) - (k_1 q_2)(k_2 l)(q_1 l) + (k_1 q)(k_2 q_1)(q_2 q) - (k_1 l)(k_2 q_1)(q_2 l) \\ & \left. \left. - (k_1 q)(k_2 q)(q_1 q_2) + (k_1 l)(k_2 l)(q_1 q_2) \pm m_N^2 ((k_1 q)(k_2 q) - (k_1 l)(k_2 l)) \right] \right. \\ & + 2 (m_N^2 - m_W^2)(m_N^2 - 2m_W^2)^2 \left[(k_1 q)(q_2 q) - (k_1 l)(q_2 l) + (k_2 q)(q_1 q) - (k_2 l)(q_1 l) \right] \\ & \left. + 8 m_W^2 (m_N^2 - m_W^2)^2 \left[(q_1 q)(q_2 q) - (q_1 l)(q_2 l) \right] \right) \\ & - 2f_2 \cdot (m_N^2 - m_W^2)(m_N^4 - 4m_W^4) \left(\pm (k_1 q)(q_1 l) - (k_1 q)(q_2 l) \right. \\ & \mp (k_1 l)(q_1 q) + (k_1 l)(q_2 q) \pm (k_2 q)(q_2 l) - (k_2 q)(q_1 l) \\ & \left. \mp (k_2 l)(q_2 q) + (k_2 l)(q_1 q) \right) \left. \right\} . \end{aligned} \quad (3.4)$$

If the final state is e^+e^+ instead of e^-e^- , we replace $f_2 \rightarrow -f_2$ in the above equation.

The expression for $|\overline{\mathcal{M}}_{\pm}|^2$ can be integrated over the phase space of W^+ and W^- (i.e. over the momenta $k_3(= q_1 - k_1)$ and $k_4(= q_2 - k_2)$), in order to obtain the spectra in the lepton variables k_1 and k_2 . Defining the four-vectors k_1 and k_2 in the e^+e^- c.m. frame by

$$\begin{aligned} k_1^\mu &= E_1 (1, \sin \theta_1 \cos \phi_1, \sin \theta_1 \sin \phi_1, \cos \theta_1) \ , \\ k_2^\mu &= E_2 (1, \sin \theta_2 \cos \phi_2, \sin \theta_2 \sin \phi_2, \cos \theta_2) \ , \end{aligned} \quad (3.5)$$

we have been able to derive the correlated distribution of the energies E_1 and E_2 , as well as the correlation of the variables $\cos \theta_1$ and $\cos \theta_2$ measured relative to the e^- beam direction.

A. Energy Correlation

The normalized spectrum in the energies of the dilepton pair e^-e^- is ($\mathcal{E}_{1,2} = E_{1,2}/m_N$)

$$\frac{1}{\sigma} \cdot \left(\frac{d\sigma}{d\mathcal{E}_1 d\mathcal{E}_2} \right) = \mathcal{N} [a + b(\mathcal{E}_1 + \mathcal{E}_2) + c(\mathcal{E}_1 + \mathcal{E}_2)^2 - c(\mathcal{E}_1 - \mathcal{E}_2)^2] \ , \quad (3.6)$$

where \mathcal{N} is a normalization factor,

$$\mathcal{N} = [\mathcal{W}^2 \beta^2 (a + b \cdot \mathcal{W} + c \cdot \mathcal{W}^2)]^{-1} \ , \quad (3.7)$$

with $\mathcal{W} = \sqrt{s} \cdot (m_N^2 - m_W^2)/2m_N^3$, $\beta = (1 - 4m_N^2/s)^{1/2}$. The coefficients a , b , c depend on the relative CP of the $N_1 N_2$ system, and take the values

$$\begin{aligned} a^+ &= m_N^2 m_W^2 (m_N^2 - m_W^2)^2 \left(2s - \frac{(m_N^2 + 2m_W^2)^2}{2m_N^2} \right) \ , \\ b^+ &= \sqrt{s} m_N^3 (m_N^2 - 2m_W^2)^2 (m_N^2 - m_W^2) \ , \quad (\eta_{CP} = +1) \\ c^+ &= -m_N^6 (m_N^2 - 2m_W^2)^2 \ , \end{aligned} \quad (3.8)$$

$$\begin{aligned} a^- &= 2 m_W^2 (m_N^2 - m_W^2)^2 (s(s - 2m_N^2) - \frac{m_N^2}{m_W^2} (m_N^2 + 2m_W^2)^2) \ , \\ b^- &= \sqrt{s} m_N (m_N^2 - 2m_W^2)^2 (m_N^2 - m_W^2) (s - 2m_N^2) \ , \quad (\eta_{CP} = -1) \\ c^- &= -m_N^4 (m_N^2 - 2m_W^2)^2 (s - 2m_N^2) \ . \end{aligned} \quad (3.9)$$

Notice that the ratios b^+/a^+ and b^-/a^- are unequal (likewise the ratios c^+/a^+ and c^-/a^-), although $b^+/c^+ = b^-/c^-$. Thus the energy correlation of the two electrons in the final state is

different for the cases $\eta_{CP} = \pm 1$. This is illustrated in Fig. 3 for the hypothetical parameters $m_N = 500$ GeV, $\sqrt{s} = 1200$ GeV. It may be noted that the factor $f_2 = 4c_V c_A$ does not appear in the spectrum ($d\sigma/d\mathcal{E}_1 d\mathcal{E}_2$), so that the energy correlation of e^+e^+ dileptons is the same as that of e^-e^- . In the limit $\beta \rightarrow 1$ the term a^\pm dominates and the '+' and '-' cases are no more distinguishable.

B. Angular Correlation

Eq. (3.4) also allows a calculation of the correlated angular distribution of the final state e^-e^- system. Defining the angles $\theta_{1,2}$ as in Eq. (3.5), and integrating over all other variables, we find

$$\begin{aligned}
\left(\frac{d\sigma}{d\cos\theta_1 d\cos\theta_2}\right)^\pm &\sim \beta \cdot \int d\cos\theta_n \left\{ f_1 \cdot \left[\mp(m_N^2 + 2m_W^2)^2 s \cdot \mathcal{K}_1^{\theta_1} \mathcal{K}_1^{\theta_2} \right. \right. \\
&+ (m_N^2 - 2m_W^2)^2 s \cdot \left(\pm\mathcal{K}_2^{\theta_1} \mathcal{K}_2^{\theta_2} (\cos\theta_n \beta - \cos\theta_1)(\cos\theta_n \beta + \cos\theta_2) \right. \\
&+ \mathcal{K}_2^{\theta_1} \mathcal{K}_1^{\theta_2} (1 + \beta \cos\theta_n \cos\theta_1) + \mathcal{K}_1^{\theta_1} \mathcal{K}_2^{\theta_2} (1 - \beta \cos\theta_n \cos\theta_2) \left. \right) \\
&+ 2m_W^2 s^2 \cdot \mathcal{K}_1^{\theta_1} \mathcal{K}_1^{\theta_2} (1 + \cos^2\theta_n \beta^2) - 4m_N^2 (m_N^2 - 2m_W^2)^2 \\
&\left. \cdot \mathcal{K}_2^{\theta_1} \mathcal{K}_2^{\theta_2} (1 - \cos\theta_1 \cos\theta_2) \right] \\
&+ f_2 \cdot 2(m_N^4 - 4m_W^4) s \cdot \left[\begin{array}{l} \cos\theta_n \beta (\mathcal{K}_2^{\theta_1} \mathcal{K}_1^{\theta_2} - \mathcal{K}_1^{\theta_1} \mathcal{K}_2^{\theta_2}) \quad : \quad + \\ \mathcal{K}_2^{\theta_1} \mathcal{K}_1^{\theta_2} \cos\theta_1 + \mathcal{K}_1^{\theta_1} \mathcal{K}_2^{\theta_2} \cos\theta_2 \quad : \quad - \end{array} \right] \left. \right\} , \quad (3.10)
\end{aligned}$$

with

$$\mathcal{K}_1^{\theta_{1(2)}} = \frac{2A_{1(2)}}{(A_{1(2)}^2 - B_{1(2)}^2)^{3/2}} , \quad \mathcal{K}_2^{\theta_{1(2)}} = \frac{2A_{1(2)}^2 + B_{1(2)}^2}{(A_{1(2)}^2 - B_{1(2)}^2)^{5/2}} , \quad (3.11)$$

$$A_{1(2)} = 1 - (+)\beta \cos\theta_n \cos\theta_{1(2)} , \quad B_{1(2)} = \beta \sin\theta_n \sin\theta_{1(2)} .$$

The correlation (3.10) has been evaluated for $m_N = 500$ GeV and $\sqrt{s} = 1200$ GeV (using $f_1 = 1 + 4\sin^2\theta_W + 8\sin^4\theta_4$, $f_2 = 1 - 4\sin^2\theta_W$) and is plotted in Fig. 4. There is a clear difference between the cases $\eta_{CP} = \pm 1$. The angular correlation in (3.10) becomes particularly transparent near the threshold $\beta \rightarrow 0$, where we obtain the analytic results

$$\frac{1}{\sigma^+} \cdot \left(\frac{d\sigma}{d \cos \theta_1 d \cos \theta_2} \right)_{\beta \rightarrow 0}^+ \approx \frac{1}{4} \cdot \left[1 + \frac{1}{2} \cdot \frac{f_2}{f_1} \cdot \frac{m_N^2 - 2m_W^2}{m_N^2 + 2m_W^2} \cdot (\cos \theta_1 + \cos \theta_2) \right], \quad (3.12)$$

$$\begin{aligned} \frac{1}{\sigma^-} \cdot \left(\frac{d\sigma}{d \cos \theta_1 d \cos \theta_2} \right)_{\beta \rightarrow 0}^- \approx \frac{1}{4} \cdot \left[1 + \frac{(m_N^2 - 2m_W^2)^2}{(m_N^2 + 2m_W^2)^2} \cdot \cos \theta_1 \cos \theta_2 \right. \\ \left. + \frac{f_2}{f_1} \cdot \frac{(m_N^2 - 2m_W^2)}{(m_N^2 + 2m_W^2)} \cdot (\cos \theta_1 + \cos \theta_2) \right]. \end{aligned} \quad (3.13)$$

Notice that the distribution in the variables $\cos \theta_1$ and $\cos \theta_2$ becomes flat in the case $\eta_{CP} = +1$ when f_2/f_1 is neglected. By contrast, there remains a nontrivial correlation for $\eta_{CP} = -1$, even in the absence of f_2 . As before, the above results for e^-e^- hold for e^+e^+ if one replaces $f_2 \rightarrow -f_2$.

IV. UNLIKE-SIGN DILEPTONS: THE REACTION $e^+e^- \rightarrow N_1N_2 \rightarrow W^+W^-e^+e^-$

Proceeding as in Sec. 3, the matrix element for the reaction $e^+e^- \rightarrow N_1N_2 \rightarrow W^+W^-e^+e^-$ (Fig. 2) is

$$\begin{aligned} \mathcal{M}_m = iA \ j_\mu^e \ \Delta_Z^{\mu\nu} \frac{1}{q_1^2 - m_1^2 + im_1\Gamma_1} \cdot \frac{1}{q_2^2 - m_2^2 + im_2\Gamma_2} \cdot \\ \left[\lambda_2 \bar{u}_{t_1}(k_1) \gamma_\rho \not{q}_1 \gamma_\nu \not{q}_2 \gamma_\sigma \frac{1}{2}(1 - \gamma_5) v_{t_2}(k_2) \right. \\ \left. + \lambda_1 m_1 m_2 \bar{u}_{t_1}(k_1) \gamma_\rho \gamma_\nu \gamma_\sigma \frac{1}{2}(1 - \gamma_5) v_{t_2}(k_2) \right] \epsilon_{\lambda_3}^{*\rho}(k_3) \epsilon_{\lambda_4}^{*\sigma}(k_4) . \end{aligned} \quad (4.1)$$

The same final state, produced via a Dirac particle-antiparticle pair ($e^+e^- \rightarrow N\bar{N} \rightarrow W^+W^-e^+e^-$), has the amplitude

$$\begin{aligned} \mathcal{M}_d = iA \ j_\mu^e \ \Delta_Z^{\mu\nu} \frac{1}{q_1^2 - m_1^2 + im_1\Gamma_1} \cdot \frac{1}{q_2^2 - m_2^2 + im_2\Gamma_2} \cdot \\ \bar{u}_{t_1}(k_1) \gamma_\rho \not{q}_1 \gamma_\nu \not{q}_2 \gamma_\sigma \frac{1}{2}(1 - \gamma_5) v_{t_2}(q_2) \epsilon_{\lambda_3}^{*\rho}(k_3) \epsilon_{\lambda_4}^{*\sigma}(k_4) . \end{aligned} \quad (4.2)$$

Summing (averaging) over final (initial) polarizations, and using the narrow-width approximation for the N_1, N_2 propagators, we obtain the squared matrix elements given below:

$$\overline{|\mathcal{M}_\pm|^2} = \frac{|A|^2}{2} \frac{1}{(s - m_Z^2)^2} \frac{\pi}{m_N \Gamma_n} \delta(q_1^2 - m_N^2) \frac{\pi}{m_N \Gamma_n} \delta(q_2^2 - m_N^2) \frac{m_N^2}{m_W^4} .$$

$$\begin{aligned}
& \left\{ f_1 \cdot \left(\mp(m_N^2 - m_W^2)^2(m_N^2 + 2m_W^2)^2 \cdot s \pm 4(m_N^2 - 2m_W^2)^2 \cdot \right. \right. \\
& \quad \left[s(k_1 k_2)(q_1 q_2) - s(k_1 q_2)(k_2 q_1) - (k_1 k_2)(q_1 q)(q_2 q) + (k_1 k_2)(q_1 l)(q_2 l) \right. \\
& \quad + (k_1 q_2)(k_2 q)(q_1 q) - (k_1 q_2)(k_2 l)(q_1 l) + (k_1 q)(k_2 q_1)(q_2 q) - (k_1 l)(k_2 q_1)(q_2 l) \\
& \quad \left. \left. - (k_1 q)(k_2 q)(q_1 q_2) + (k_1 l)(k_2 l)(q_1 q_2) \pm m_N^2 ((k_1 q)(k_2 q) - (k_1 l)(k_2 l)) \right] \right. \\
& \quad \left. - 2(m_N^2 - m_W^2)(m_N^2 - 2m_W^2)^2 \left[(k_1 q)(q_2 q) - (k_1 l)(q_2 l) + (k_2 q)(q_1 q) - (k_2 l)(q_1 l) \right] \right. \\
& \quad \left. + 2(m_N^2 + 4m_W^2/m_N^2)(m_N^2 - m_W^2)^2 \left[(q_1 q)(q_2 q) - (q_1 l)(q_2 l) \right] \right) \\
& - 2f_2 \cdot \left((m_N^2 - m_W^2)(m_N^4 - 4m_W^4) \left(\pm(k_1 q)(q_1 l) - (k_1 q)(q_2 l) \right. \right. \\
& \quad \mp(k_1 l)(q_1 q) + (k_1 l)(q_2 q) \mp(k_2 q)(q_2 l) + (k_2 q)(q_1 l) \\
& \quad \left. \pm(k_2 l)(q_2 q) - (k_2 l)(q_1 q) \right) \\
& \quad \left. + 2(m_N^2 + 4m_W^4/m_N^2)(m_N^2 - m_W^2)^2 \left[(q_1 q)(q_2 l) - (q_2 q)(q_1 l) \right] \right) \left. \right\} , \tag{4.3}
\end{aligned}$$

$$\begin{aligned}
\overline{|\mathcal{M}_d|^2} &= |A|^2 \frac{1}{(s - m_Z^2)^2} \frac{\pi}{m_N \Gamma_n} \delta(q_1^2 - m_N^2) \frac{\pi}{m_N \Gamma_n} \delta(q_2^2 - m_N^2) \\
& \left\{ f_1 \cdot \left(\frac{m_N^4}{m_W^4} (m_N^2 - 2m_W^2)^2 \cdot \left[(k_1 q)(k_2 q) - (k_1 l)(k_2 l) \right] \right. \right. \\
& \quad + 2 \frac{m_N^2}{m_W^2} (m_N^2 - m_W^2)(m_N^2 - 2m_W^2) \cdot \left[(k_1 q)(q_2 q) - (k_1 l)(q_2 l) + (k_2 q)(q_1 q) - (k_2 l)(q_1 l) \right] \\
& \quad \left. + 4(m_N^2 - m_W^2)^2 \cdot \left[(q_1 q)(q_2 q) - (q_1 l)(q_2 l) \right] \right) \\
& + f_2 \cdot \left(\frac{m_N^4}{m_W^4} (m_N^2 - 2m_W^2)^2 \cdot \left[(q_1 q)(k_2 l) - (k_2 q)(k_1 l) \right] \right. \\
& \quad + 2 \frac{m_N^2}{m_W^2} (m_N^2 - m_W^2)(m_N^2 - 2m_W^2) \cdot \left[(k_1 q)(q_2 l) - (k_2 q)(q_1 l) + (q_1 q)(k_2 l) - (q_2 q)(k_1 l) \right] \\
& \quad \left. \left. + 4(m_N^2 - m_W^2)^2 \cdot \left[(q_1 q)(q_2 l) - (q_2 q)(q_1 l) \right] \right) \right\} . \tag{4.4}
\end{aligned}$$

In complete analogy with the discussion of like-sign leptons (Sec. 3), we derive from the above equations the correlation in the energies and angles of the final e^+e^- state.

A. Energy Correlation

The distribution in the scaled energies $\mathcal{E}_1, \mathcal{E}_2$ has the quadratic form given in Eq. (3.6), where the coefficients in the Majorana cases '+' and '-' and the Dirac case 'd' now have

the values

$$\begin{aligned}
a^+ &= \frac{1}{2} m_N^2 (m_N^2 - m_W^2)^2 \left(\frac{s}{m_N^2} (m_N^4 + 4m_W^4) - 2(m_N^2 + 2m_W^2)^2 \right) , \\
b^+ &= -\sqrt{s} m_N^3 (m_N^2 - 2m_W^2)^2 (m_N^2 - m_W^2) , \\
c^+ &= m_N^6 (m_N^2 - 2m_W^2)^2 , \\
a^- &= \frac{1}{2} m_N^2 (m_N^2 - m_W^2)^2 \left(s(s - 2m_N^2) \left(1 + 4 \frac{m_W^4}{m_N^4} \right) - 4(m_N^2 + 2m_W^2)^2 \right) , \\
b^- &= -\sqrt{s} m_N (m_N^2 - 2m_W^2)^2 (m_N^2 - m_W^2) (s - 2m_N^2) , \\
c^- &= m_N^4 (m_N^2 - 2m_W^2)^2 (s - 2m_N^2) , \\
a^d &= (m_N^2 - m_W^2)^2 \left(4(s - m_N^2)(s - 4m_N^2) \frac{m_W^4}{m_N^2} \right. \\
&\quad \left. - (m_N^2 - 2m_W^2) \left(2(s - 4m_N^2)m_W^2 - m_N^2(m_N^2 - 2m_W^2) \right) \right) , \\
b^d &= \sqrt{s} m_N (m_N^2 - 2m_W^2) (m_N^2 - m_W^2) \left(4sm_W^2 - (m_N^2 + 14m_W^2)m_N^2 \right) , \\
c^d &= m_N^4 (m_N^2 - 2m_W^2)^2 (s - 3m_N^2) . \tag{4.5}
\end{aligned}$$

The corresponding three distributions are plotted in Fig. 5. As in the case of like-sign dileptons, the e^+e^- pairs have distinct correlations for $\eta_{CP} = \pm 1$. A comparison of the Majorana cases with the Dirac case reveals an interesting difference. In the Majorana cases the total e^+e^- energy $Y = \mathcal{E}_1 + \mathcal{E}_2$ is distributed symmetrically around the mid-point of this variable $Y_0 = 1/2(Y_{min} + Y_{max})$. By contrast, e^+e^- pairs resulting from Dirac $N\bar{N}$ primary state have a total energy distribution that is unsymmetric around the mid-point.

B. Angle Correlation

In analogy to the distribution $d\sigma/d \cos \theta_1 d \cos \theta_2$ obtained for e^-e^- pairs (Eq. 3.10), the result for unlike-sign dileptons e^+e^- is

$$\begin{aligned}
\left(\frac{d\sigma}{d \cos \theta_1 d \cos \theta_2} \right)^\pm &\sim \beta \cdot \int d \cos \theta_n \left\{ f_1 \cdot \right. \\
&\left[\mp 2m_N^2 (m_N^2 + 2m_W^2)^2 s \cdot \mathcal{K}_1^{\theta_1} \mathcal{K}_1^{\theta_2} \right. \\
&\left. - 2m_N^2 (m_N^2 - 2m_W^2)^2 s \cdot \left(\pm \mathcal{K}_2^{\theta_1} \mathcal{K}_2^{\theta_2} (\cos \theta_n \beta - \cos \theta_1) (\cos \theta_n \beta + \cos \theta_2) \right) \right]
\end{aligned}$$

$$\begin{aligned}
& + \mathcal{K}_2^{\theta_1} \mathcal{K}_1^{\theta_2} (1 + \beta \cos \theta_n \cos \theta_1) + \mathcal{K}_1^{\theta_1} \mathcal{K}_2^{\theta_2} (1 - \beta \cos \theta_n \cos \theta_2)) \\
& + (m_N^4 + 4m_W^4) s^2 \cdot \mathcal{K}_1^{\theta_1} \mathcal{K}_1^{\theta_2} (1 + \cos^2 \theta_n \beta^2) + 8m_N^4 (m_N^2 - 2m_W^2)^2 \cdot \\
& \quad \mathcal{K}_2^{\theta_1} \mathcal{K}_2^{\theta_2} (1 - \cos \theta_1 \cos \theta_2)] \\
& + f_2 \cdot 2(m_N^4 - 4m_W^4) s \cdot \left[-\mathcal{K}_1^{\theta_1} \mathcal{K}_1^{\theta_2} \cdot s \cos \theta_n \beta \right. \\
& \quad \left. + 2m_N^2 \cdot \left[\begin{array}{l} \cos \theta_n \beta (\mathcal{K}_2^{\theta_1} \mathcal{K}_1^{\theta_2} + \mathcal{K}_1^{\theta_1} \mathcal{K}_2^{\theta_2}) \quad : \quad + \\ \mathcal{K}_2^{\theta_1} \mathcal{K}_1^{\theta_2} \cos \theta_1 - \mathcal{K}_1^{\theta_1} \mathcal{K}_2^{\theta_2} \cos \theta_2 \quad : \quad - \end{array} \right] \right] \left. \right\} , \tag{4.6}
\end{aligned}$$

$$\begin{aligned}
\left(\frac{d\sigma}{d \cos \theta_1 d \cos \theta_2} \right)^d & \sim \beta \cdot \int d \cos \theta_n \left\{ f_1 \cdot \right. \\
& \left[s^2 m_W^4 \cdot \mathcal{K}_1^{\theta_1} \mathcal{K}_1^{\theta_2} \cdot (1 + \cos \theta_n \beta^2) \right. \\
& + m_N^2 m_W^2 (m_N^2 - 2m_W^2) s \cdot \left(\mathcal{K}_2^{\theta_1} \mathcal{K}_2^{\theta_2} (1 + \beta \cos \theta_n \cos \theta_1) + \mathcal{K}_1^{\theta_1} \mathcal{K}_2^{\theta_2} (1 - \beta \cos \theta_n \cos \theta_2) \right) \\
& + m_N^4 (m_N^2 - 2m_W^2)^2 \cdot \mathcal{K}_2^{\theta_1} \mathcal{K}_2^{\theta_2} \cdot (1 - \cos \theta_1 \cos \theta_2) \left. \right] \\
& + f_2 \cdot \left[2s^2 m_W^4 \cdot \mathcal{K}_1^{\theta_1} \mathcal{K}_1^{\theta_2} \cdot \cos \theta_n \beta \right. \\
& + m_N^2 m_W^2 (m_N^2 - 2m_W^2) s \cdot \left(\mathcal{K}_2^{\theta_1} \mathcal{K}_2^{\theta_2} (\cos \theta_n \beta + \cos \theta_1) + \mathcal{K}_1^{\theta_1} \mathcal{K}_2^{\theta_2} (\cos \theta_n \beta - \cos \theta_2) \right) \\
& \left. \left. + m_N^4 (m_N^2 - 2m_W^2)^2 \cdot \mathcal{K}_2^{\theta_1} \mathcal{K}_2^{\theta_2} \cdot (\cos \theta_1 - \cos \theta_2) \right] \right\} . \tag{4.7}
\end{aligned}$$

As usual, the indices '+', '-' and 'd' differentiate between the Majorana cases $\eta_{CP} = +1$, -1 and the Dirac case. The angle-correlations expressed by Eqs. (4.6), (4.7) are plotted in Fig. 6., where the differences between the three cases are obvious. Close to threshold ($\beta \rightarrow 0$), the correlation between $\cos \theta_1$ and $\cos \theta_2$ can be presented in analytic form

$$\frac{1}{\sigma^+} \cdot \left(\frac{d\sigma}{d \cos \theta_1 d \cos \theta_2} \right)_{\beta \rightarrow 0}^+ \approx \frac{1}{4} \cdot \left[1 + \frac{1}{2} \cdot \frac{f_2}{f_1} \cdot \frac{m_N^2 - 2m_W^2}{m_N^2 + 2m_W^2} \cdot (\cos \theta_1 - \cos \theta_2) \right] , \tag{4.8}$$

$$\frac{1}{\sigma^d} \cdot \left(\frac{d\sigma}{d \cos \theta_1 d \cos \theta_2} \right)_{\beta \rightarrow 0}^d = \frac{1}{\sigma^-} \cdot \left(\frac{d\sigma}{d \cos \theta_1 d \cos \theta_2} \right)_{\beta \rightarrow 0}^- \tag{4.9}$$

$$\approx \frac{1}{4} \cdot \left[1 - \frac{(m_N^2 - 2m_W^2)^2}{(m_N^2 + 2m_W^2)^2} \cdot \cos \theta_1 \cos \theta_2 + \frac{f_2}{f_1} \cdot \frac{(m_N^2 - 2m_W^2)}{(m_N^2 + 2m_W^2)} \cdot (\cos \theta_1 - \cos \theta_2) \right] .$$

In this limit, the cases '+' and '-' remain distinct, but the case $\eta_{CP} = -1$ converges to the Dirac case.

V. COMMENTS

We comment briefly on some other papers which have a partial overlap with the considerations presented above.

- (i) Our discussion of the production reaction $e^+e^- \rightarrow N_1N_2$ follows very closely that given in Ref. [1]. Our results for $d\sigma/d\Omega$ given in the Appendix (Eqs. (A.1)–(A.6)) essentially coincide with those in this paper, with two minor differences: The angular distributions for the case of two distinct Majorana particles with the same CP -parity, as well as for the case of two distinct Dirac particles (Eq. (4E) and (4D) in Ref. [1]), are slightly different from our distributions, presented in the Appendix (Eq. (A.2) and (A.3)).
- (ii) The cross section for the Majorana process $e^+e^- \rightarrow N_1N_2$, with $m_1 = m_2$ and $\eta_{CP} = +1$ calculated in Ref. [2] agrees with that obtained in this paper. However the Dirac case $e^+e^- \rightarrow N\bar{N}$ (Eq. (2) of Ref. [2]) differs from our result (Eq. (A.5)), as also noted in Ref. [1].
- (iii) The spin-summed differential cross section for the Majorana process $e^+e^- \rightarrow N_1N_2$ (with $m_1 = m_2$, $\eta_{CP} = +1$) calculated in the present paper, as well as in Refs. [1,2], differs from that given in Ref. [4], but agrees with the results given in Refs. [3,6,10].
- (iv) Our analysis of heavy Majorana production and decay has been essentially model-independent. Discussions in the context of specific gauge models, based on $SU(2)_L \times SU(2)_R \times U(1)$ or $E(6)$ symmetries, may be found in Refs. [6,10,11].

APPENDIX A: DIFFERENTIAL CROSS SECTION FOR $e^+e^- \rightarrow N_1N_2$

Following Ref. [1], we consider the following five cases, in which N_1 and N_2 are

- A** distinct Dirac particles.
- B** distinct Majorana particles with the same CP -parity.
- C** distinct Majorana particles with opposite CP -parity.
- D** Dirac particle-antiparticle pair.
- E** identical Majorana particles.

Choosing the N_1 direction in the e^+e^- c.m. system to be the z-axis, and the e^- -beam direction to be at an angle θ (= scattering angle), the momenta (q_1, q_2) and spins (t_1, t_2) of N_1 and N_2 have components

$$\begin{aligned}
 N_1 : q_1^\mu &= (\gamma m_1, 0, 0, \gamma \beta m_1) \quad , \\
 t_1^\mu &= (\gamma \beta n_z, n_x, n_y, \gamma n_z) \quad , \\
 N_2 : q_2^\mu &= (\gamma' m_2, 0, 0, -\gamma' \beta' m_2) \quad , \\
 t_2^\mu &= (-\gamma' \beta' n'_z, n'_x, n'_y, \gamma' n'_z) \quad .
 \end{aligned} \tag{A.1}$$

The differential cross sections are (with $\beta = (1 - 4m_1^2/s)^{1/2}$, $\beta' = (1 - 4m_2^2/s)^{1/2}$, $\gamma = (1 - \beta^2)^{-1/2}$, $\gamma' = (1 - \beta'^2)^{-1/2}$, $\lambda(x, y, z) = [x^2 + y^2 + z^2 - 2(xy + yz + zx)]^{1/2}$)

$$\begin{aligned}
 \left(\frac{d\sigma}{d\Omega}\right)_A &= \frac{G_F^2 \alpha_N^2}{512\pi^2} |R(s)|^2 [1 - (m_1^2 - m_2^2)^2/s^2] \lambda(s, m_1^2, m_2^2) \\
 &\quad \left\{ f_1 [(1 + C^2 \beta' \beta) - (\beta n'_z + \beta' n_z)(1 + C^2) - (\beta' n_x/\gamma + \beta n'_x/\gamma') SC \right. \\
 &\quad \quad \left. + n_z n'_z (C^2 + \beta \beta') + (n_x n'_z/\gamma + n'_x n_z/\gamma') SC + n_x n'_x S^2/\gamma \gamma'] \right. \\
 &\quad \left. + f_2 [C(\beta + \beta') - (n_z + n'_z)C(1 + \beta \beta') - (n_x/\gamma + n'_x/\gamma') S \right. \\
 &\quad \left. + n_z n'_z C(\beta + \beta') + S(\beta' n_x n'_z/\gamma + \beta n'_x n_z/\gamma')] \right\} \quad ,
 \end{aligned} \tag{A.2}$$

$$\begin{aligned}
\left(\frac{d\sigma}{d\Omega}\right)_B &= \frac{G_F^2 \alpha_N^2}{256\pi^2} |R(s)|^2 [1 - (m_1^2 - m_2^2)^2/s^2] \lambda(s, m_1^2, m_2^2) \\
&\left\{ f_1 [n_x n'_x S^2(1/\gamma\gamma' - 1) + n_y n'_y S^2 \beta\beta' + n_z n'_z (\beta\beta' - C^2(1/\gamma\gamma' - 1)) \right. \\
&\quad \left. + (n_x n'_z - n'_x n_z) SC(1/\gamma - 1/\gamma') + C^2 \beta\beta' - 1/\gamma\gamma' + 1 \right] \\
&+ f_2 [(n_x - n'_x) S(1/\gamma' - 1/\gamma) + (n_z + n'_z) C(1/\gamma\gamma' - \beta\beta' - 1)] \left. \right\}, \quad (\text{A.3})
\end{aligned}$$

$$\begin{aligned}
\left(\frac{d\sigma}{d\Omega}\right)_C &= \frac{G_F^2 \alpha_N^2}{256\pi^2} |R(s)|^2 [1 - (m_1^2 - m_2^2)^2/s^2] \lambda(s, m_1^2, m_2^2) \\
&\left\{ f_1 [n_x n'_x S^2(1/\gamma\gamma' + 1) - n_y n'_y S^2 \beta\beta' + n_z n'_z (\beta\beta' + C^2(1/\gamma\gamma' + 1)) \right. \\
&\quad \left. + (n_x n'_z + n'_x n_z) SC(1/\gamma + 1/\gamma') + C^2 \beta\beta' + 1/\gamma\gamma' + 1 \right] \\
&- f_2 [(n_x + n'_x) S(1/\gamma + 1/\gamma') + (n_z + n'_z) C(1/\gamma\gamma' + \beta\beta' + 1)] \left. \right\}, \quad (\text{A.4})
\end{aligned}$$

$$\begin{aligned}
\left(\frac{d\sigma}{d\Omega}\right)_D &= \left(\frac{d\sigma}{d\Omega}\right)_{A, m_1=m_2} = \frac{G_F^2 \alpha_N^2}{512\pi^2} |R(s)|^2 \lambda(s, m^2, m^2) \\
&\left\{ f_1 [(1 + C^2 \beta^2) - (n_z + n'_z) \beta(1 + C^2) - (n_x + n'_x) SC\beta/\gamma + n_z n'_z (C^2 + \beta^2) \right. \\
&\quad \left. + (n_x n'_z + n_z n'_x) SC/\gamma + n_x n'_x S^2/\gamma^2] + f_2 [2C\beta - (n_z + n'_z) C(1 + \beta^2) \right. \\
&\quad \left. - (n_x + n'_x) S/\gamma + 2n_z n'_z C\beta + (n_x n'_z + n'_x n_z) S\beta/\gamma \right] \left. \right\}, \quad (\text{A.5})
\end{aligned}$$

$$\begin{aligned}
\left(\frac{d\sigma}{d\Omega}\right)_E &= \frac{1}{2} \cdot \left(\frac{d\sigma}{d\Omega}\right)_{B, m_1=m_2} = \frac{G_F^2 \alpha_N^2}{512\pi^2} |R(s)|^2 \lambda(s, m^2, m^2) \beta^2 \\
&\left\{ f_1 [(n_y n'_y - n_x n'_x) S^2 + (1 + n_z n'_z)(1 + C^2)] - f_2 2(n_z + n'_z) C \right\}. \quad (\text{A.6})
\end{aligned}$$

APPENDIX B: MATRIX ELEMENTS FOR $e^+e^- \rightarrow N_1 N_2 \rightarrow e^\pm e^- W^\mp W^+$

1. Like Sign Dileptons

The matrix element for the reaction (Fig. 2)

$$e^+(p_2, t_2) + e^-(p_1, t_1) \rightarrow e^-(k_1) e^-(k_2) W^+(k_3, \lambda_3) W^+(k_4, \lambda_4) \quad (\text{B.1})$$

is

$$\begin{aligned}
\mathcal{M} = iA j_\mu^e \Delta_Z^{\mu\nu} \left\{ \lambda_2 \bar{u}_{t_1}(k_1) \gamma_\rho \frac{1}{2}(1 - \gamma_5) \frac{\not{q}_1 + m_1}{q_1^2 - m_1^2 + im_1\Gamma_1} \gamma_\nu \frac{1}{2}(1 - \gamma_5) \right. \\
\left. \frac{-\not{q}_2 + m_2}{q_2^2 - m_2^2 + im_2\Gamma_2} \gamma_\sigma \frac{1}{2}(1 + \gamma_5) v_{t_2}(k_2) \right. \\
- \lambda_1 \bar{u}_{t_2}(k_2) \gamma_\sigma \frac{1}{2}(1 - \gamma_5) \frac{\not{q}_2 + m_2}{q_2^2 - m_2^2 + im_2\Gamma_2} \gamma_\nu \frac{1}{2}(1 - \gamma_5) \\
\left. \frac{-\not{q}_1 + m_1}{q_1^2 - m_1^2 + im_1\Gamma_1} \gamma_\rho \frac{1}{2}(1 + \gamma_5) v_{t_1}(k_1) \right\} \epsilon_{\lambda_3}^{*\rho}(k_3) \epsilon_{\lambda_4}^{*\sigma}(k_4) . \quad (\text{B.2})
\end{aligned}$$

Upon rearrangement, this gives the matrix element in Eq. (3.2).

2. Unlike Sign Dileptons

The matrix element for the Majorana-mediated process (Fig. 2)

$$e^+(p_2, t_2) + e^-(p_1, t_1) \rightarrow e^-(k_1) e^-(k_2) W^+(k_3, \lambda_3) W^+(k_4, \lambda_4) \quad (\text{B.3})$$

is

$$\begin{aligned}
\mathcal{M}_m = -iA j_\mu^e \Delta_Z^{\mu\nu} \left\{ \lambda_2 \bar{u}_{t_1}(k_1) \gamma_\rho \frac{1}{2}(1 - \gamma_5) \frac{\not{q}_1 + m_1}{q_1^2 - m_1^2 + im_1\Gamma_1} \gamma_\nu \frac{1}{2}(1 - \gamma_5) \right. \\
\left. \frac{-\not{q}_2 + m_2}{q_2^2 - m_2^2 + im_2\Gamma_2} \gamma_\sigma \frac{1}{2}(1 - \gamma_5) v_{t_2}(k_2) \right. \\
- \lambda_1 \bar{u}_{t_1}(k_1) \gamma_\rho \frac{1}{2}(1 - \gamma_5) \frac{\not{q}_1 + m_1}{q_1^2 - m_1^2 + im_1\Gamma_1} \gamma_\nu \frac{1}{2}(1 + \gamma_5) \\
\left. \frac{-\not{q}_2 + m_2}{q_2^2 - m_2^2 + im_2\Gamma_2} \gamma_\sigma \frac{1}{2}(1 - \gamma_5) v_{t_2}(k_2) \right\} \epsilon_{\lambda_3}^{*\rho}(k_3) \epsilon_{\lambda_4}^{*\sigma}(k_4) . \quad (\text{B.4})
\end{aligned}$$

Upon rearrangement, this gives the matrix element in Eq. (4.1).

REFERENCES

- [1] J. Kogo, S.Y. Tsai, Prog. Theor. Phys. 86, 183 (1991)
- [2] E. Ma, J. Pantaleone, Phys. Rev. D 40, 2172 (1989)
- [3] J. Maalampi, K. Mursula, R. Vuopionperä, Nucl. Phys. B 372, 23 (1992)
- [4] M.J. Duncan, P. Langacker, Nucl. Phys. B 275, 285 (1986)
- [5] A. Denner et al., Nucl. Phys. B 387, 467 (1992)
- [6] W. Buchmüller, C. Greub, Nucl. Phys. B 381, 109 (1992)
and Nucl. Phys. B 363, 345 (1991)
- [7] R.N. Mohapatra, P.B. Pal, "Massive Neutrinos in Physics and Astrophysics", World Scientific (1991)
- [8] B. Kayser et al., "The Physics of Massive Neutrinos", World Scientific (1989)
- [9] B. Kayser, Phys. Rev. D 30 1023 (1984)
- [10] F.D. Aguila, E. Laermann, P. Zerwas, Nucl. Phys. B 297, 1 (1988)
- [11] J. Gluza, M. Zralek, Phys. Rev. D 48, 5093 (1993)

FIGURE CAPTIONS

1. Feynman diagram for the reaction $e^+e^- \rightarrow N_1N_2$
2. Diagram showing the sequential process $e^+e^- \rightarrow N_1N_2 \rightarrow e^\pm e^- W^\mp W^+$
3. Energy correlation of the e^-e^- lepton pair in the reaction $e^+e^- \rightarrow N_1N_2 \rightarrow e^-W^+e^-W^+$, for the cases (a) $\eta_{CP} = +1$, (b) $\eta_{CP} = -1$. (Parameters for this and succeeding figures: $\sqrt{s} = 1.2$ TeV, $m_N = 500$ GeV.)
4. Angle correlation of e^-e^- dileptons in $e^+e^- \rightarrow N_1N_2 \rightarrow e^-W^+e^-W^+$, for (a) $\eta_{CP} = +1$, (b) $\eta_{CP} = -1$
5. Energy correlation of e^-e^+ dileptons in $e^+e^- \rightarrow N_1N_2 \rightarrow e^-W^+e^+W^-$: (a) Majorana pair, $\eta_{CP} = +1$, (b) Majorana pair, $\eta_{CP} = -1$, (c) Dirac $N\bar{N}$ -pair
6. Angle correlation of e^-e^+ dileptons in $e^+e^- \rightarrow N_1N_2 \rightarrow e^-W^+e^+W^-$: (a) Majorana pair, $\eta_{CP} = +1$, (b) Majorana pair, $\eta_{CP} = -1$, (c) Dirac $N\bar{N}$ -pair

FIGURES

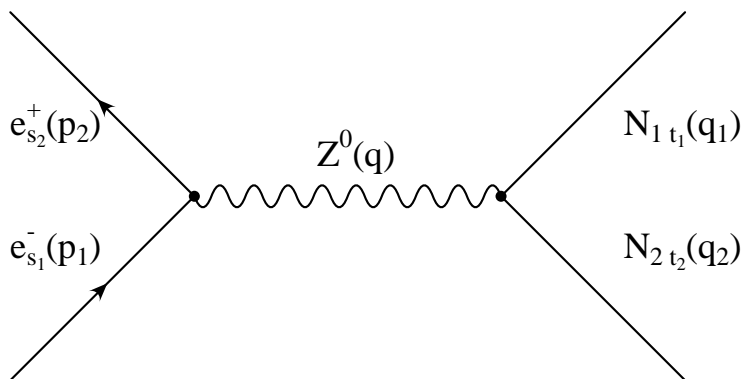


FIG. 1.

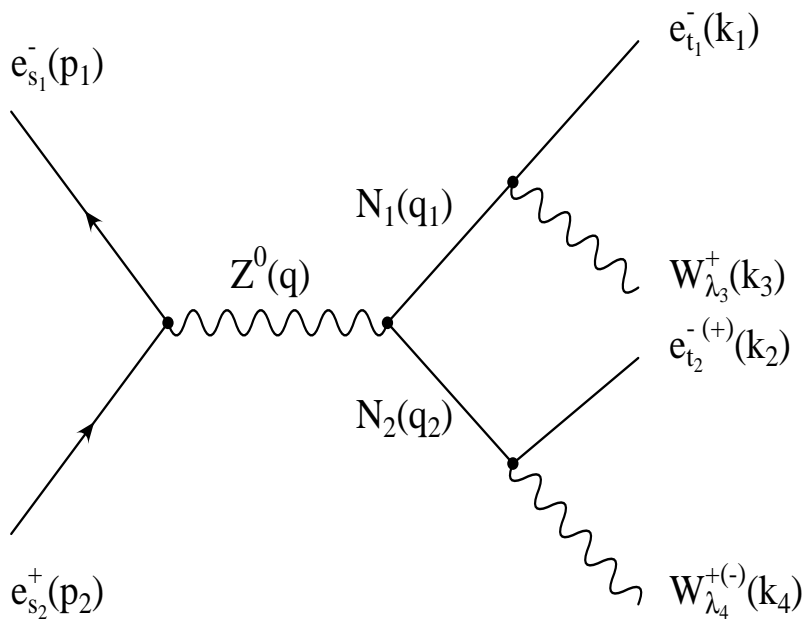


FIG. 2.

e^-e^- Final State: Energy Correlation

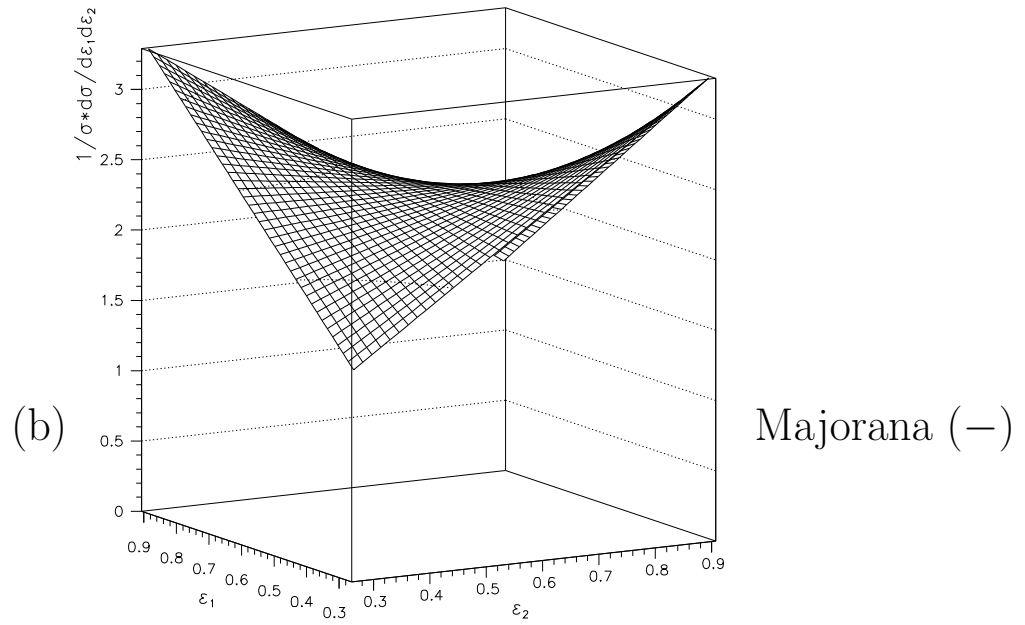
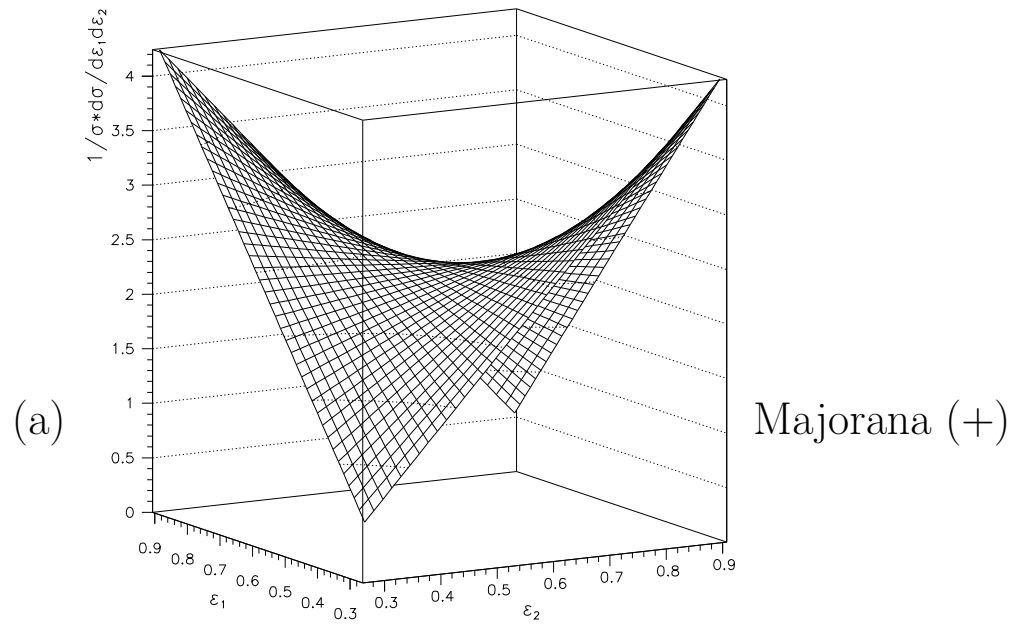


FIG. 3.

e^-e^- Final State: Angular Correlation

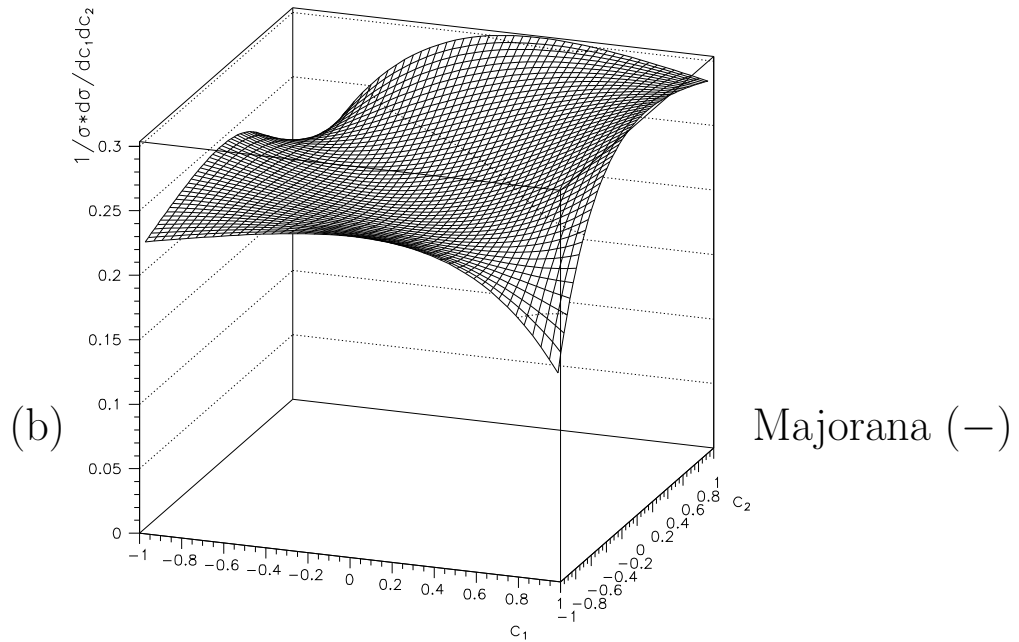
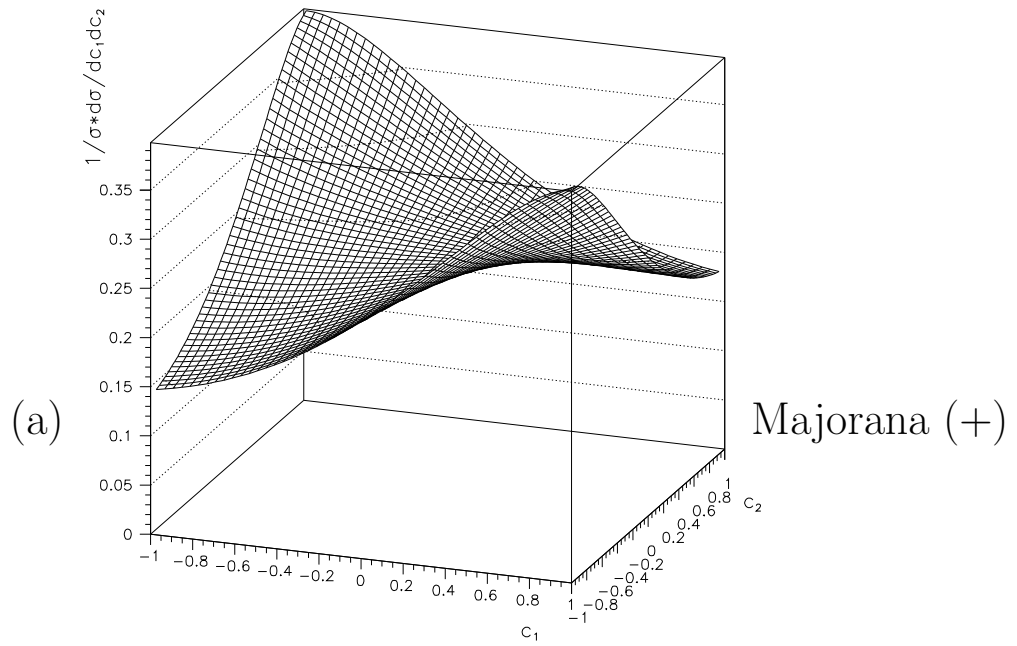
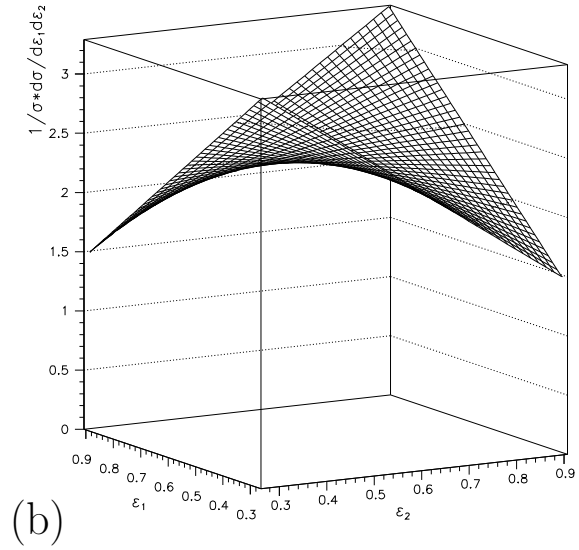
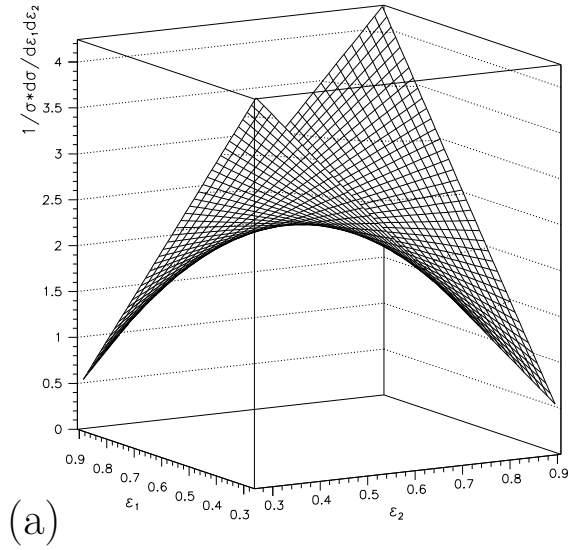


FIG. 4.

e^+e^- Final State: Energy Correlation

Majorana (+)

Majorana (-)



Dirac

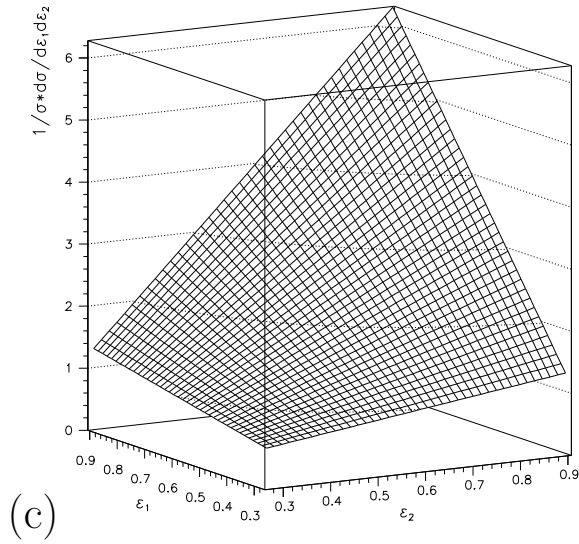
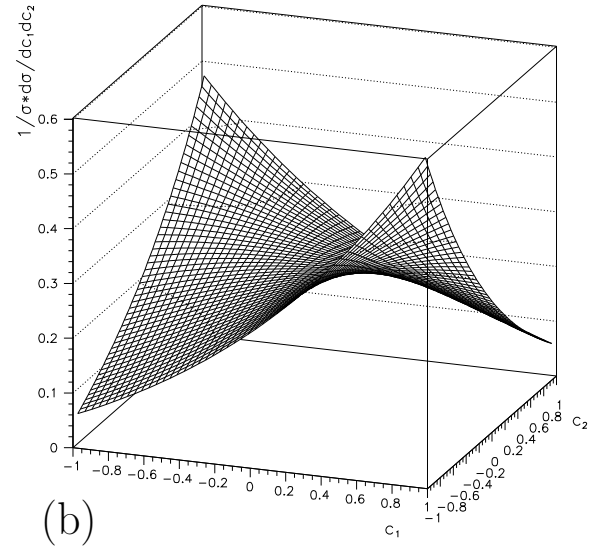
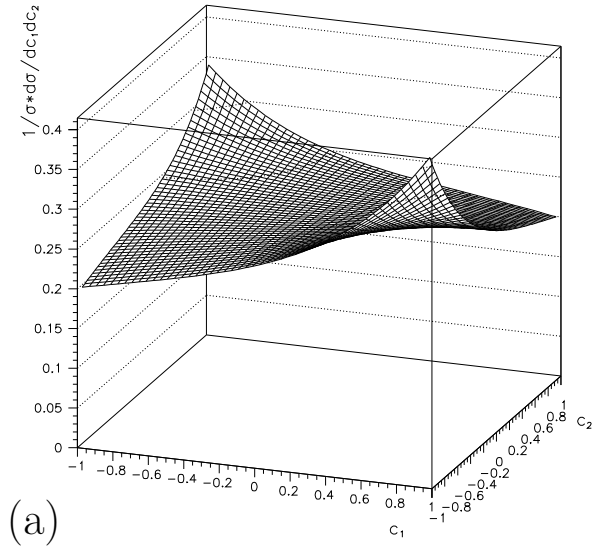


FIG. 5.

e^+e^- Final State: Angular Correlation

Majorana (+)

Majorana (-)



Dirac

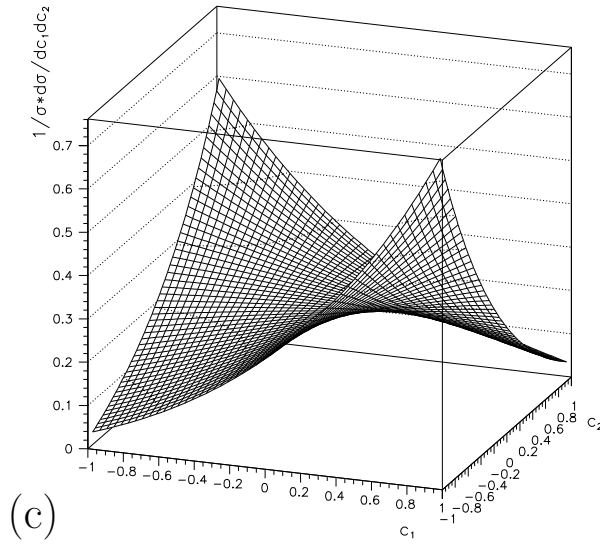


FIG. 6.